Comparison of Modeled and Measured Performance of GSO Crystal as Gamma Detector

D. S. Parno[a,b,*], M. Friend[a,c], V. Mamyan[a], F. Benmokhtar[a,1], A. Camsonne[d], G. B. Franklin[a], K. Paschke[e], B. Quinn[a]

[a] *Carnegie Mellon University, Department of Physics, Pittsburgh, PA 15213, USA*
[b] *University of Washington, Center for Experimental Nuclear Physics and Astrophysics and Department of Physics, Seattle, WA 98195, USA*
[c] *High Energy Accelerator Research Organization (KEK), Tsukuba, Ibaraki, Japan*
[d] *Thomas Jefferson National Accelerator Facility, Newport News, VA 23606, USA*
[e] *University of Virginia, Department of Physics, Charlottesville, VA 22904, USA*

Abstract

We have modeled, tested, and installed a large, cerium-activated Gd_2SiO_5 crystal scintillator for use as a detector of gamma rays up to 600 MeV. We present the measured detector response to two types of incident photons: nearly monochromatic photons up to 40 MeV, and photons from a continuous Compton backscattering spectrum up to 600 MeV. Our GEANT4 simulations reproduce the measured spectra well.

Keywords: GSO, Geant4

1. Introduction

Cerium-activated gadolinium oxyorthosilicate (Gd_2SiO_5:Ce, or GSO) [1] is a scintillator with a high light output and fast decay time relative to many other commonly used crystals, *e.g.* $Bi_4Ge_3O_{12}$ (BGO). These properties, along with the crystal's non-hygroscopic nature, its relative ease of growth, and its radiation hardness, have made it a popular choice for a number of detection applications. Its most high-profile use is in positron emission tomography [2], where detectors are optimized for 511-keV photons, but GSO scintillators have also been used to detect protons [3], charged leptons, and pions [4].

In 2009, a GSO crystal with Ce:0.5 mol% doping, grown by Hitachi Chemical and read out with a photomultiplier tube (PMT), was adopted as a gamma detector for the upgraded Compton polarimeter [5] in Hall A [6] of the Thomas Jefferson National Accelerator Facility (Jefferson Lab) [7]. This device exploits Compton scattering to make a continuous measurement of the longitudinal electron-beam polarization, a vital parameter for a significant portion of Hall A's experimental program. Integration of the energy that backscattered photons deposit in this crystal allows such a measurement to be made with accuracy better than 1% [5]. Depending on the beam energy chosen for the experiment (1 – 6 GeV), the maximum energy of a Compton-backscattered photon may range from 34 MeV to 1 GeV.

Uncertainties in the detector response to incident gammas are important potential sources of systematic error, especially if the response is non-linear. To reduce these uncertainties, a model was developed using the GEANT4 simulation toolkit [8] and was compared to calibration data, taken at two facilities, with incident gammas from 20 to 600 MeV. Section 2 describes the Compton polarimeter and the fundamental simulation method as applied to single-arm Compton photon data at Jefferson Lab. Section 3 discusses further tests at Jefferson Lab using photons tagged by coincident Compton-scattered electrons. In Section 4, we give the results of tests at the High-Intensity γ Source (HIγS) [9] with nearly monoenergetic photon beams in the 20 – 40-MeV range.

2. Simulation Method and Test with Single Photons at Jefferson Lab

In the Compton polarimeter in the Hall A beamline at Jefferson Lab, the polarized electron beam is routed through a four-dipole magnetic chicane. In the center of the chicane, the beam passes through circularly polarized laser light in a high-finesse Fabry-Pérot cav-

*Corresponding author. dparno@uw.edu
[1] Present address: Duquesne University, Pittsburgh, PA 15282, USA

ity. Compton-backscattered photons pass through the third dipole undeflected; the GSO calorimeter is located on this direct path. A silicon-microstrip detector (Section 3), located above the third dipole, detects Compton-scattered electrons, which are deflected through a larger angle than the unscattered majority of the beam. The Fabry-Pérot cavity is periodically taken out of resonance, eliminating Compton-scattering events in the cavity and allowing a direct background measurement. During typical running, the dipole fields are controlled via feedback from a beam-position monitor in the chicane, so as to maintain a stable beam position.

Light from the GSO calorimeter is collected in a 2-inch, 12-stage PMT, with a base customized for maximum linearity of response. The data-acquisition system is based on a 200-MHz, 12-bit Struck SIS3320 flash analog-to-digital converter, modified to integrate the input signal over an externally timed window. In addition to performing this onboard integration, the SIS3320 card records all samples from the window in one of two internal buffers. Timestamps from photon- or electron-detector triggers, recorded in a CAEN V830 latching scaler, allow the retention of some information about individual pulses. For a prescaled sample of pulses, the numerical sum of samples from the programmable readout window is recorded in the datastream; the energy of the incident photon can be retrieved from this pulse integral. For a smaller number of pulses, all of the samples for the readout window are written to disk, allowing pulse-shape analysis [5]. It is also possible to trigger the system at regular intervals that are uncorrelated with photon pulses, allowing the study of pileup events. These triggers are generated either in software or with a remotely programmable function generator.

The GEANT4 Monte Carlo (MC) simulation of the GSO crystal response begins with the generation of a beam of simulated photons to match the experimental beam. To reproduce a Compton-backscattered beam, simulated photons of various energies are generated with probabilities weighted by the Compton scattering cross-section for the specific kinematics (i.e. initial electron and laser-photon energies) of the planned experiment. The simulated photons are then allowed to interact with items in the beamline; in the standard Hall A installation, this includes a 1-mm-thick, 4-cm-diameter lead filter and a 5-cm-thick, 8-cm-diameter lead collimator with an interchangeable aperture up to 2 cm in diameter. The final item in the beamline is the GSO crystal, a cylinder 6 cm in diameter and 15 cm (10.9 radiation lengths) long; Table 1 lists the other crystal properties used in the MC. Figure 1 histograms the locations where photons in the simulation first interact with matter. GEANT4 modeling of the gamma shower relies on the cross-section σ for gamma conversion into an (e^+, e^-) pair; for gamma energies between 1.5 MeV and 100 GeV, the parameterization is accurate to within 5%, with a mean accuracy of 2.2% [10]. Electromagnetic interactions are modeled based on the Livermore physics list; hadronic interactions are based on the QGSP_BIC physics list. The combined non-linearity of the photomultiplier tube and front-end electronics was determined empirically [11], and the resulting functional form is an input to the simulation.

An optical extension to this basic simulation follows the path of each scintillation photon produced in the electromagnetic shower from an incident Compton-scattered photon. This package approximates the polished GSO surface as perfectly smooth, and includes the aluminum-foil detector wrapping (with a modeled reflectivity of 0.9) and the efficiency of the PMT photocathode. The output of the MC is the number of photoelectrons produced in the simulated photocathode. The

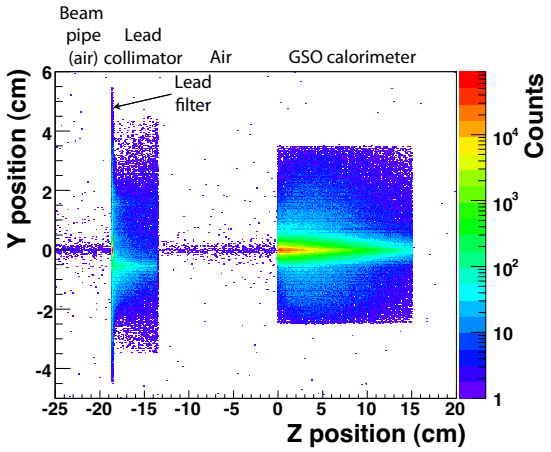

Figure 1: Histogram of positions of the first interaction point of incident photons in the Hall A Compton gamma beamline, as determined by the GEANT4 MC. The z axis is the central axis of the incident Compton-scattered photons; the y axis is vertical. In this figure, the central axis of the calorimeter and the 2-cm aperture of the collimator is offset by 0.5 cm from the gamma beam, reflecting conditions during one run period.

Property	Value	Reference
Density	6.71 g/cm^3	[12]
Radiation length	1.38 cm	[3]
Attenuation length	340 cm	estimated from [3]
Birks' constant	5.25 μm/MeV	[13]

Table 1: GSO:Ce (0.5 mol%) properties used in simulation

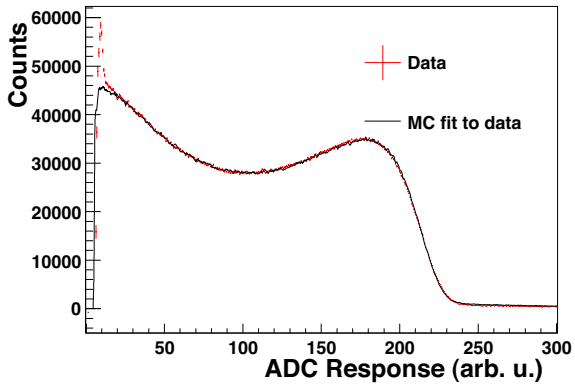

Figure 2: A Compton spectrum measured in Hall A, with the ADC response given in arbitrary units. The Compton edge in this configuration was at 204 MeV. A non-optical MC with 2.3% Gaussian smearing is fit to the experimental data with only two free parameters: a horizontal scale factor and a vertical scale factor. The discrepancy at low photon energies is an artifact of an anomaly in the trigger threshold; this region is excluded from the fit.

resulting spectrum shows non-Gaussian smearing due to optical effects such as shower leakage from the crystal and the dependence of photon-collection efficiency on the initial interaction position. However, the computational cost of this package is prohibitive for some simulation tasks.

Spectra simulated under Jefferson-Lab conditions must be modified to take into account pileup, in which two or more pulses arrive and are integrated during the readout window for a single trigger. This correction is determined experimentally based on periodically triggered snapshots of the readout window, which give the random-event rate and the spectrum of energy deposited by random pulses during such a window. For spectra from electron-photon coincidence data (Section 3), it is sufficient to use this spectrum to add random, pileup pulse integrals to those of simulated Compton-scattered photons. For photon-arm singles data, however, the correction is complicated by the possibility of pileup between two Compton events; a naive pileup correction would count such a pair twice. This double-counting effect is canceled by a careful construction of the empirical pileup spectrum that is added to the MC: half from dedicated background measurements and half from Compton-scattering data [14]. For simulations of the primary running mode, in which signals are integrated over a long, untriggered window, no pileup correction is necessary.

A 2.3% Gaussian smearing function must be folded into the basic, non-optical MC for a satisfactory match

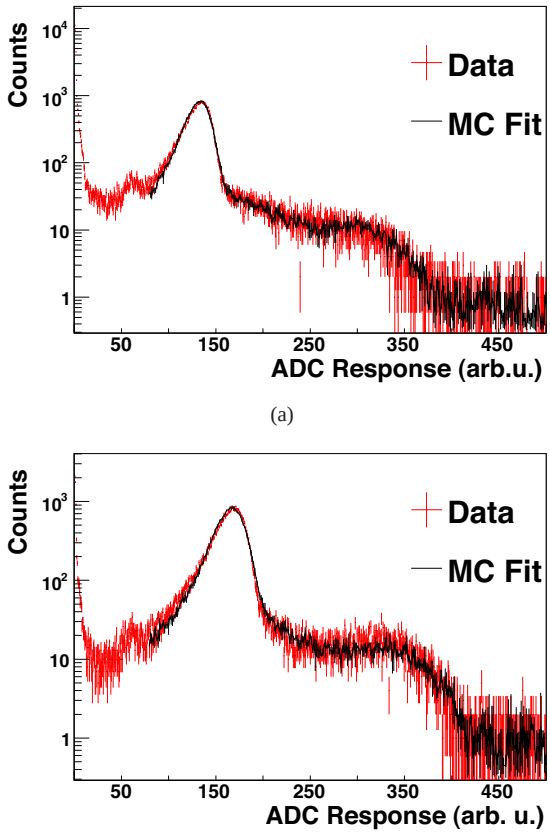

Figure 3: Fits of the non-optical MC, including background, to tagged photon spectra from (a) strip 10 (125.1 – 127.0-MeV photons, χ^2/dof = 2.13) and (b) strip 21 (158.5 – 160.4-MeV photons, χ^2/dof = 2.33).

to the experimental data, as shown in Fig. 2. By contrast, the optical MC requires only 1.5% Gaussian smearing; that is, a 1.5% smearing is not accounted for by modeled optical effects. At high data rates, pileup corrections are necessary for both models.

3. Tests with Tagged Photons at Jefferson Lab

Further tests of the GSO calorimeter in Hall A were performed with photons tagged by the electron detector located above the third dipole of the Compton polarimeter. Each of this detector's four planes consists of 192 horizontal strips with a 240-μm pitch. When a scattered electron strikes the detector, the vertical position of the strip gives its deflection angle in the third dipole and therefore its momentum, which in turn determines the energy of the associated scattered photon. The electron

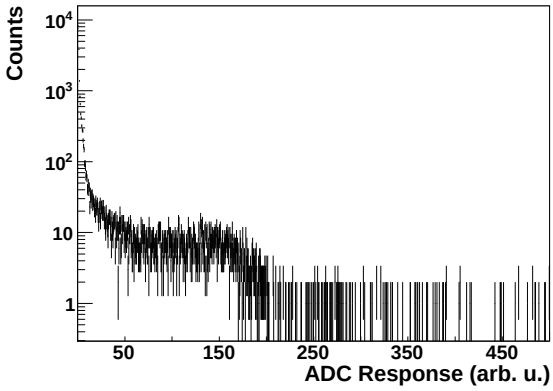

Figure 4: Measured spectrum of pileup pulses in tagged-photon data, used to correct MC spectra.

detector can thus tag the energies of coincident photons seen in the GSO crystal. For these data, taken with an initial electron-beam energy of 3.4 GeV, only the bottom 37 strips saw Compton-scattered electrons.

Figure 3 shows measured and modeled spectra of photons tagged by two typical strips. GSO readout was triggered by the electron detector. Due to computational constraints, the MC is non-optical, but it does include simulated background events and pileup effects; Fig. 4 shows the measured pileup spectrum used for the MC. Each fit has three free parameters: a vertical scale factor, a horizontal scale factor, and a factor setting the amount of included background. The latter varies from strip to strip because electron-detector noise, which is slightly different for each strip, is a significant source of background. MC fits for all 37 strips are given a common horizontal offset and 5% Gaussian smearing; the larger smearing requirement is likely due to poorly understood effects in the electron detector.

4. Tests with 20 – 40-MeV Photons at HIγS

HIγS produces a 2- to 65-MeV gamma beam via Compton scattering. At HIγS, electron bunches that circulate in a storage ring are sent through magnetic undulators, causing the electrons to produce free-electron laser (FEL) light, which is stored in an optical cavity. The FEL photons are then allowed to collide with electrons in the storage ring; the Compton-backscattered photons travel through a manually adjustable collimator. The result is a nearly monoenergetic gamma beam in the experimental hall, approximately 60 m downstream of the Compton interaction point.

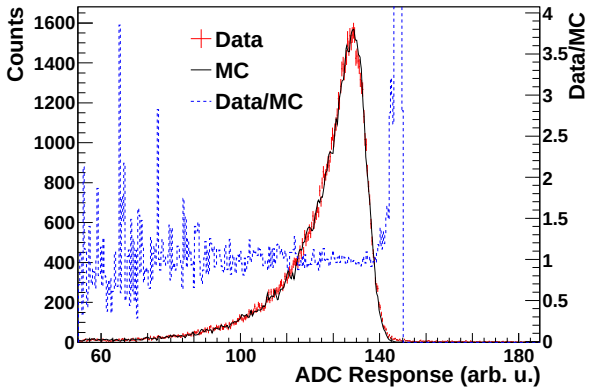

(a)

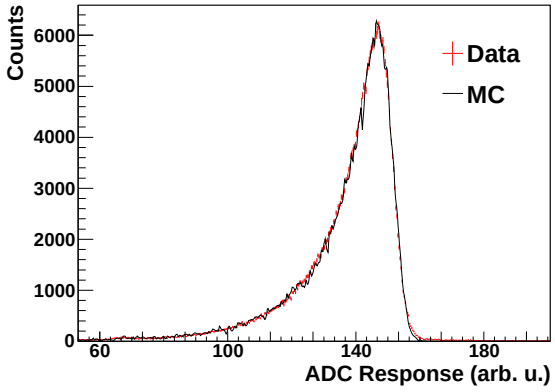

(b)

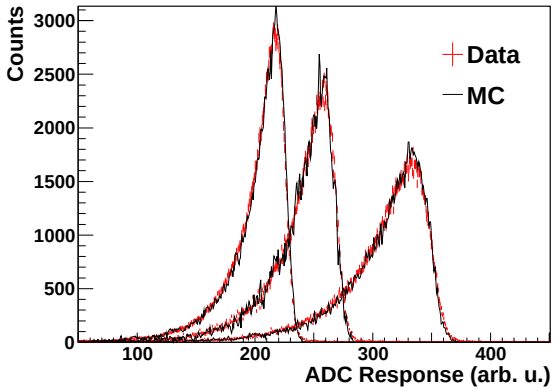

(c)

Figure 5: Simulated spectra fit with two free parameters (horizontal and vertical scale factors) to experimental data from the HIγS facility, for incident photons at (a) 20 MeV (χ^2/dof = 3.26, plotted with the ratio of measured counts to simulated counts (dashed line)), (b) 22 MeV (χ^2/dof = 10.97), and (c) 25, 30, and 40 MeV, with a combined fit for all three energies (χ^2/dof = 10.20). Gain shifts prevent combining the fits to the 20- and 22-MeV spectra.

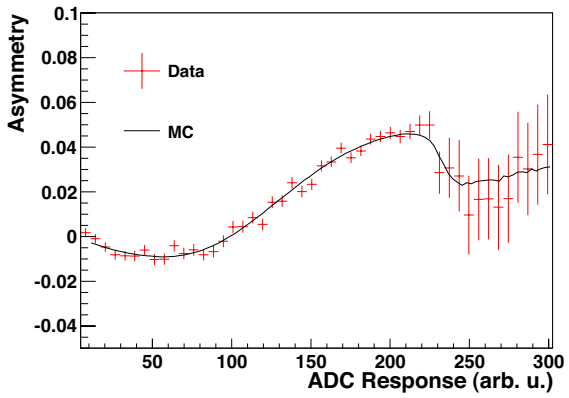

Figure 6: The measured Compton asymmetry plotted as a function of ADC response to deposited photon energy. The experimental data are compared to GEANT4 MC data with no adjustable parameters. The Compton edge in this configuration was at 204 MeV.

A series of HIγS-beam test runs at five different photon energies (20, 22, 25, 30, and 40 MeV) was taken using the GSO calorimeter; gain shifts after the 20-MeV and 22-MeV data points prevent the analysis of all five energies together. Figure 5 shows the measured spectra at these energies, as well as the ratio of measured to modeled counts for 20-MeV photons. An optical MC of the HIγS configuration, including non-linearity, was fit to each spectrum with two free parameters: horizontal and vertical scale factors. Background and pileup effects were negligible at all energies except 22 MeV, and were not included in the MC.

Because the energy spread of the HIγS beam is well known, fits to these data constrain the minimum amount of additional smearing that must be included to bring the MC into agreement with the data. The corresponding 1.5% smearing is included in the simulations shown in Fig. 5.

5. Conclusion

We have demonstrated agreement at the few-percent level between the MC of this GSO:Ce crystal and photon spectra measured over a range of rates and energies. The ultimate purpose of the MC, however, was to unfold the detector response from Compton-photon polarimetry data in Hall A. The asymmetry in Compton-scattering cross-sections for opposite photon-and-electron spin configurations is proportional to the polarizations of both incident beams and to the analyzing power of the apparatus [5]; the MC is a vital input to the latter. Figure 6 shows the measured Compton asymmetry as a function of the energy deposited in the GSO by Compton-scattered photons. The non-optical MC result is plotted on the same axes with no adjustable parameters. The horizontal scale was determined from a fit to the full photon energy spectrum (Fig. 2); the vertical scale is set by the electron beam polarization, which was confirmed by Møller polarimetry measurements [15], and by the incident photon polarization.

With the aid of this MC, the analyzing power for the GSO calorimeter is known to within 0.33%; this uncertainty is dominated by the 0.3% error on the detector non-linearity measurement [5]. Existing GEANT4 physics modules allow simulation of the GSO:Ce response to gammas in the 20 – 600-MeV energy range with satisfactory precision.

We gratefully acknowledge the assistance of staff and scientists at HIγS, especially Mohammad Ahmed, Sean Stave, and Ying Wu, and at Jefferson Lab, especially the Hall A Compton laser working group. This work was supported by DOE grant DE-FG02-87ER40315.

References

[1] K. Takagi, T. Fukazawa, Appl. Phys. Lett. 42 (1983) 43–45.
[2] J. L. Humm, A. Rosenfeld, A. Del Guerra, Eur. J. Nucl. Med. Mol. Imaging 30 (2003) 1574–1597.
[3] Y. Tamagawa, et al., Nucl. Inst. & Meth. in Phys. Res. A 562 (2006) 120–126.
[4] M. Kobayashi, et al., Nucl. Inst. & Meth. in Phys. Res. A 306 (1991) 139 – 144.
[5] M. Friend, et al., Nucl. Inst. & Meth. in Phys. Res. A 676 (2012) 96–105.
[6] J. Alcorn, et al., Nucl. Inst. & Meth. in Phys. Res. A 522 (2004) 294–346.
[7] C. W. Leemann, D. R. Douglas, G. A. Krafft, Annu. Rev. Nucl. Part. Sci. 51 (2001) 413–450.
[8] S. Agostinelli, et al., Nucl. Inst. & Meth. in Phys. Res. A 506 (2003) 250–303.
[9] H. R. Weller, et al., Prog. Part. Nucl. Phys. 62 (2009) 257–303.
[10] GEANT4 Physics Reference Manual, 9.5 edition, 2011.
[11] M. Friend, G. B. Franklin, B. Quinn, Nucl. Inst. & Meth. in Phys. Res. A 676 (2012) 66–69.
[12] C. L. Melcher, et al., IEEE Trans. Nucl. Sci. 37 (1990) 161–164.
[13] V. Avdeichikov, et al., Nucl. Inst. & Meth. in Phys. Res. A 439 (2000) 158.
[14] M. Friend, A Precision Measurement of the Proton Strange-Quark Form Factors at $Q^2 = 0.624\,\mathrm{GeV}^2$, Ph.D. thesis, Carnegie Mellon University, 2012.
[15] Z. Ahmed, et al., Phys. Rev. Lett. 108 (2012) 102001.